



Fast Multi-Wavelength Pyrometer for Dynamic Temperature Measurements

R. Belikov¹ · D. Merges¹ · D. Varentsov² · Zs. Major^{2,3} · P. Neumayer² · Ph. Hesselbach^{2,4} · M. Schanz² · B. Winkler¹

Received: 15 November 2023 / Accepted: 23 December 2023 / Published online: 1 February 2024
© The Author(s) 2024

Abstract

Multi-wavelength pyrometry is an efficient tool for measuring high temperatures in dynamic experiments. A fast 5-channel pyrometer was built and successfully employed in ion-beam heating experiments at the GSI Centre for Heavy Ion Research (Darmstadt, Germany). Temperatures of metallic samples heated by an intense focused heavy ion beam up to their melting points and beyond were measured with nanosecond time resolution and a spatial resolution of about 200 μm . The modular instrument has demonstrated its high versatility also for temperature measurements of exothermic reactions with millisecond temporal resolution.

Keywords Heavy-ion heating · Pyrometry · Temperature measurement

1 Introduction

Non-contact temperature measurements in the range of up to several thousand Kelvin are a challenging experimental problem. The pyrometrical determination of surface temperatures by collecting and analyzing thermal radiation is one of the few practically reliable methods for temperature measurements in this range [1]. The brightness temperatures are obtained by absolute measurements of the emitted

Selected Papers of the 22nd European Conference on Thermophysical Properties.

✉ R. Belikov
belikov@kristall.uni-frankfurt.de

¹ Institute of Geosciences, Goethe-University Frankfurt am Main, Altenhoferallee 1, 60438 Frankfurt am Main, Germany

² GSI Helmholtz Centre for Heavy Ion Research, Planckstrasse 1, 64291 Darmstadt, Germany

³ Helmholtz Institut Jena, Fröbelstieg 3, 07741 Jena, Germany

⁴ Institute for Applied Physics, Goethe-University Frankfurt am Main, Max-von-Laue Str. 1, 60438 Frankfurt am Main, Germany

thermal radiation in a specific wavelength regime, and by fitting the recorded signals to Planck's law.

Multi-spectral pyrometers are divided into multi-wavelength (using several monochromatic channels) and multi-band (using wide-band channels) systems [2]. The light emission of a sample is typically described by a set of equations with a given number of variables which need to be determined experimentally. Depending on the set-up and the mathematical model, the set of equations can be solved either analytically or by fitting. Generally, intensity determinations in narrow wavelengths bands, which are well separated from each other, spread across a broad frequency spectrum, and sample the lower wavelengths sufficiently well, provide more accurate solutions. The subsequent data analysis strongly relies on the relationship between emissivity and wavelength, which is, in turn, strongly dependent on the characteristics of a particular surface. Depending on the object properties, the expected temperature range, and the process dynamics different multi-spectral techniques will be optimal.

In multi-wavelength pyrometry, the radiance of a hot source is measured at several wavelengths, and, employing certain assumptions about the spectral and temperature dependencies of the emissivity, the true temperature of the sample can then be deduced [3].

For the “constant emissivity” assumption, the light intensity values at different wavelengths can be transformed into so-called Wien coordinates: the independent variable plotted on the horizontal axis is $\frac{c_2}{\lambda}$, while the vertical axis shows $\ln(\lambda^5 I)$. Here $c_2 = 1.4388 \times 10^4 \mu\text{m K}$ is the second radiation constant, λ is the wavelength and I is the light intensity. The slope of the straight line in these coordinates defines the true temperature of the material under the assumption of constant emissivity.

For the “linear emissivity” model, a set of N equations with N variables is constructed, one for each wavelength λ_i and, for example, in the case of three channels $N = 3$. The variables are the true temperature T and the coefficients a and b for the linear dependence of the emissivity, so that:

$$\ln(I\lambda_i^5) = -\frac{c_2}{\lambda_i T} + \ln(c_1(a + b\lambda_i)), \quad (1)$$

where $c_1 = 1.1910 \times 10^8 \text{ W} \cdot \mu\text{m}^4 \cdot \text{m}^{-2} \cdot \text{sr}^{-1}$ is the first radiation constant. This set of equations can be solved numerically, e.g., by the Levenberg–Marquardt algorithm. Increasing the number of channels, so that intensities are recorded at more wavelengths generally helps to overcome the limitations of the constant and linear emissivity models.

The pyrometer described here has been developed for heavy ion irradiation experiments using the HHT (High energy, High Temperature) experimental area of the GSI Centre for Heavy Ion Research (Gesellschaft für Schwerionenforschung, Darmstadt, Germany). The main ideas of this instrument are based on earlier works [4, 5]. Several of improvements have been made to increase the sensitivity of the instrument in terms of temperature, including the integration of a new type of detector. The device has demonstrated its capability for temperature measurements in the range from about one to several thousand Kelvin in various experiments within a broad range of temporal resolution from nanoseconds to milliseconds. We were able

to measure the temperature of tungsten, tantalum, iron, and copper foils, heated by an intense focused heavy ion beam up to 1000 K–4000 K. The capability of the instrument for the characterization of exothermic reactions with millisecond time resolution was demonstrated in experiments using a pyrotechnic sparkler.

2 Description of the Instrument

2.1 Detector Set

A commonly employed approach in multi-wavelength pyrometry is to use linear photodiode arrays (PDA) or charge-coupled device (CCD) array detectors in conjunction with a spectrally selective device such as a diffraction grating. This allows to construct pyrometers with a high degree of flexibility in terms of the number of channels and covered spectral regions [6]. However, PDA and CCD detectors are not suitable for fast dynamic experiments because of their limited temporal resolution. Instead one can use fast PIN (Positive-Intrinsic-Negative) photodiodes or other fast optical detectors but only for a limited number of wavelengths (channels). The choice of the optimal number of pyrometer channels for the best accuracy of the measurements is a non-trivial problem and depends on the expected temperature range, geometrical and surface properties of the probed area, and features of the optical system. It has been suggested that using more than 10 channels is not effective [7].

For our instrument, we have decided to use five channels in each of the two independent and complementary “arms” of the spectrometer, distributed over the wavelength range from the visible to the near-infrared (450 nm–1500 nm). This design allows that the instrument can easily be adapted to different use cases according to the temperature range of interest. It is also easy to add or exchange the detectors in the different channels, thereby optimizing the system concerning the required time resolution. This is important as the sample temperature may rapidly rise in the course of a dynamic experiment, where the signal in each channel may vary by a few orders of magnitude in less than a few microseconds, while in other experiments, the temperatures will change appreciably only on the time scale of a second.

For detecting relatively slowly changing signals and low temperatures, Hamamatsu C10439-10 PIN photodiodes are used which have low-level dark-currents, about 5 μ s rise-time, and a 1 mm active zone diameter. They are installed in the channels for the near-infrared region above 1000 nm. For higher temperatures and nanosecond time resolution, we use various PIN diodes with amplifiers and multi-pixel photon counters (MPPC) which have the highest sensitivity among all common types of detectors. MPPC detectors do not require additional amplification and have the best rise time (from 0.5 to 5 ns) and linear response, which is essential for accurate measurements. Photodiodes generally have better accuracy and have a lower noise level than MPPC.

A picture of the spectral discrimination system with the respective detectors is shown in Fig. 1. The detector system is located in a control room far away from the

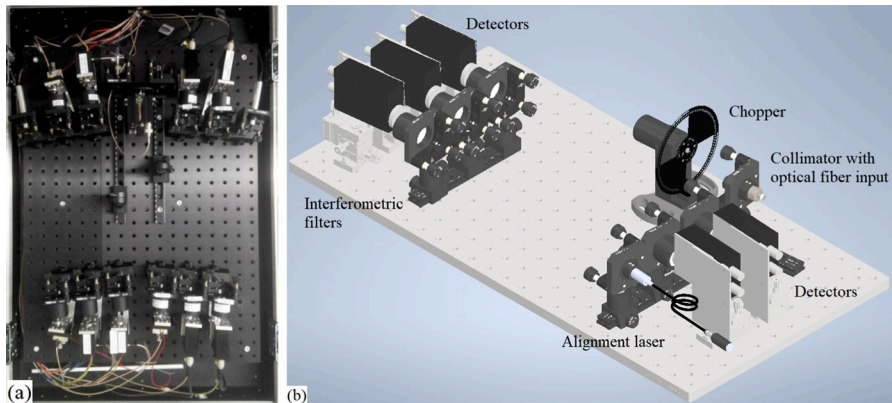


Fig. 1 Two-arms, 5×2 -channel detector system (PIN diodes and MPPCs) (a) and a drawing of one arm with fast PIN diode modules (b)

experimental area, which protects it from radiation damage, stray electromagnetic fields, and environmental temperature variations.

The initial set of detectors used in the experiments at GSI includes 3 MPPC detectors (Hamamatsu C13852-1350GA) in the “fast” arm, 3 MPPC (Hamamatsu C11209-110) in both “fast” and “slow” arms, and 4 amplified PIN photodiodes (Hamamatsu C10439-10) in the “slow” arm. After testing, the detector system has been further optimized for fast experiments by including two infrared (Femto HCA-S-400 M-IN) and three visible (Femto HCA-S-400 M-SI) PIN-diode models with a fast time response and 0 MHz–400 MHz bandwidth.

2.2 Light Collection and Transmission System

For relatively low temperatures, the efficient coupling of light into the detector system plays a crucial role. In our applications, the light collection system has to be rather compact in order to fit inside the vacuum target chamber, free from chromatic aberrations, and should provide a spatial resolution down to a few tens of micrometers. As the thermal radiation is collected and analyzed in a wide spectral range from the visible to the near-infrared, one cannot use glass lenses, and instead reflecting optics have to be employed. For the light collection, a parabolic off-axis mirror condenser is used. This scheme was chosen because of the absence of chromatic aberrations and because of the high light collection efficiency in comparison to any system of lenses with the same numerical aperture. The mounting of the mirrors efficiently solves the alignment problems (see Fig. 2). The sample is placed at one focal plane of the parabolic mirror system with a focal distance of 100 mm and a fiber or fiber array is located at the second plane. This arrangement provides a 1:1 imaging of the target’s surface and covers a solid angle of 0.2. The spatial resolution (i.e., the diameter of the region from which the emitted light is collected) is therefore completely defined by the inner diameters of the optical fibers, typically 50 μm , 100 μm , 200 μm , or 400 μm . A laser beam can be sent backward through the optical system (see

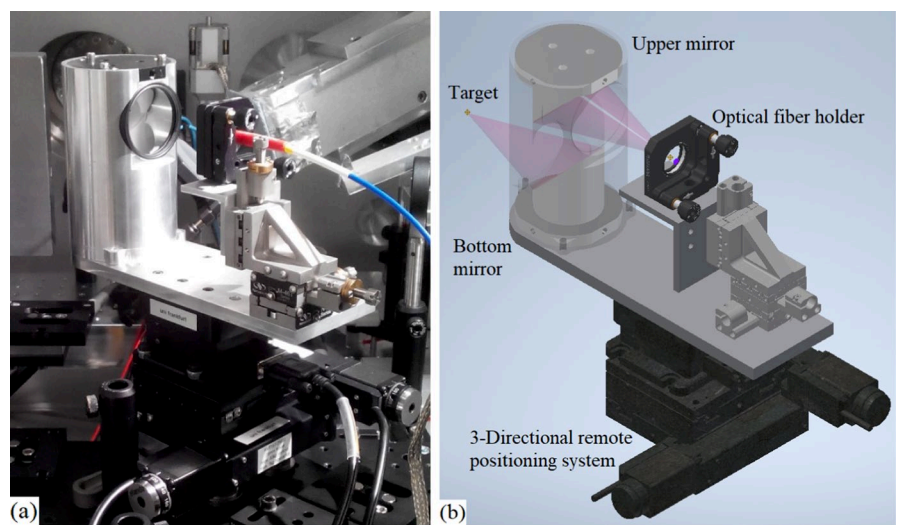


Fig. 2 The pyrometer light collection system inside the experimental vacuum chamber (a) and a drawing of this system (b)

Fig. 3), thereby facilitating the optical alignment and the location of the measuring spot. An optical chopper, which is located in front of the optical fiber ending, is used for the calibration procedure.

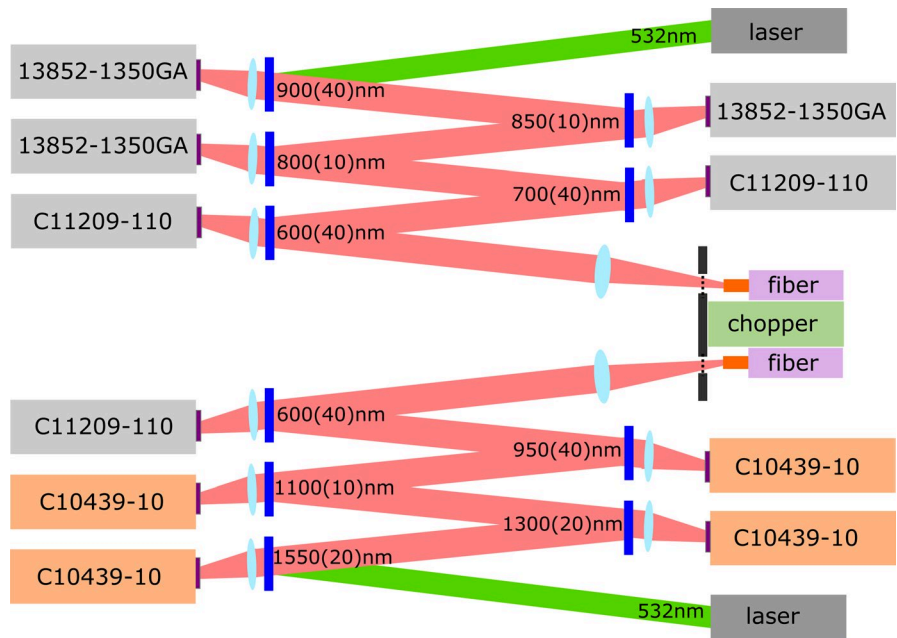


Fig. 3 Layout of the detectors system; fast arm is above, slow arm is below

2.3 Spectral Discrimination System

For spectral discrimination, a series of consecutive narrow-band interference filters is used, so the wavelengths that are not transmitted are reflected. This arrangement does not use beam splitters and is more effective than diffraction grating because of the absence of polarization. Also, this arrangement is very flexible, because the filter can be exchanged without having to exchange the detector and *vice versa*. Also, there is no interdependence between a particular filter in one wavelength range and the detectors and filters in adjacent wavelengths ranges [6].

The mounting order of the filters is chosen to provide optimal signal levels at all channels for a particular experiment, taking into account the expected temperature range, the sensitivity of detectors, and the spectral intensity of the source. For lower temperatures, relatively wide (e.g., 40 nm) interference filters are used, and therefore, the spectral ranges monitored with the available channels can not be too close to each other. The present layout of the pyrometer detector system is shown in Fig. 3.

Another set of filters was used in the ion-beam heating experiments. This set includes hard-coated bandpass filters from Thorlabs with the center wavelengths of 660(10), 780(10), 900(10), 1200(10) and 1540(12) nm (Full Width at Half Maximum bandwidths in nm inside the parentheses).

For the acquisition system, a Tektronix MSO58 oscilloscope was used. It has eight 12-bit channels, a 1 GHz bandwidth, and a sample rate of 6.25 GS/s. In later experiments, we also used a Lecroy Waverunner 8208HD oscilloscope which has similar parameters but a 2 GHz bandwidth.

3 Experimental Data

3.1 Calibration

A tungsten filament strip ribbon pharaoh-type lamp OSRAM W17/G was used for absolute calibration of the pyrometer (see Fig. 4a). This lamp is calibrated in the temperature range of 1000 K to 2300 K at 650 nm, and the brightness temperatures at other wavelengths were calculated using available data for the tungsten emissivity [8]. The calibration was done at normal incidence to the filament (target) surface both outside and inside the experimental chamber with exactly the same geometry and arrangements as during the experiment itself.

A pyrometrical calibration lamp (S6-100 by Pyrometer Inc.) (Fig. 4b) was used for the calibration for exothermic reactions experiments. This lamp is calibrated from 1073 K up to 2573 K and has a cylindrical bulb, allowing to use of different angles of view, e.g., 45°.

3.2 Heavy-Ion Heating of Metallic Foils

A set of ion-beam irradiation experiments with Ta, W, Fe, and Cu foils (100 μm thickness) was performed at the HHT experimental area of GSI-Darmstadt. Detailed

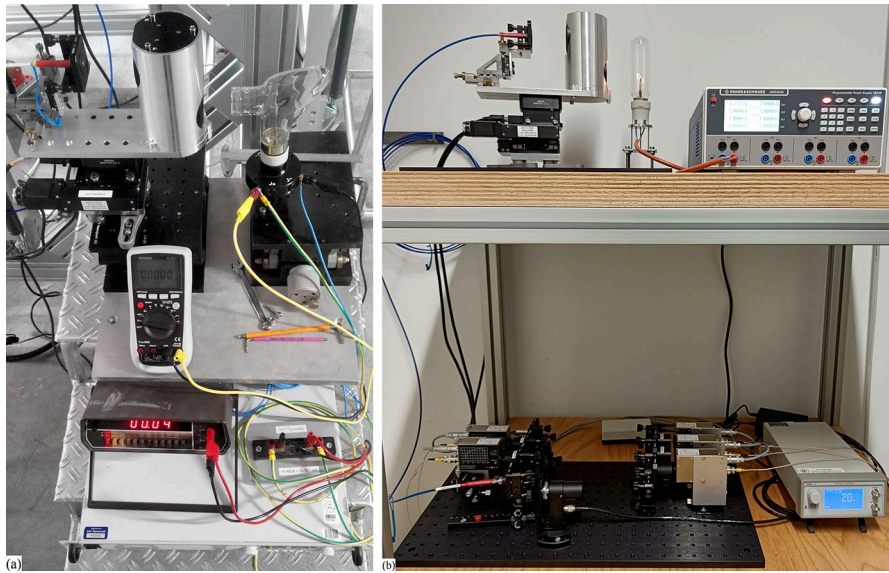


Fig. 4 Calibration of the pyrometer for the experiments at GSI (a) and for the exothermic reaction experiments at Goethe University (b)

information about these experiments will be available in a future paper under preparation (Hesselbach et al.). An intense lead ion beam accelerated in the SIS-18 heavy ion synchrotron ($E_i = 450$ MeV/u, $N \approx 4 \times 10^9$ ions) was focused to a 0.5 mm–1 mm diameter spot at the target. The pyrometer was directed at 45° to the ion-beam heated target or at a right angle, depending on the shot, while the angle between the beam and the pyrometer was always equal to 135° .

The typical brightness temperature signals of an ion-beam heated copper foil are shown in Fig. 5. The ion pulse duration was about 500 ns, followed by a slow cooling process.

3.3 Temperature Measurements for Slow Processes

A set of experiments with pyrotechnic sparklers was performed to test the capabilities of the pyrometer to measure the temperature of exothermic reactions with a millisecond time resolution. For this purpose, 4 infrared PIN diodes were used. The pyrometer measured the temperature on the sparkler surface over a $400 \mu\text{m}$ spot during its burning and subsequent cooling (see Fig. 6). First, only the brightness temperatures were measured, while emissivity behavior assumptions were applied later, in order to choose the best emissivity model. One can see the burning of the sparkler during the first second and a smooth cooling afterward. The peak visible at 2.2 s in Figs. 6 and 7 could be due to a spark passing through the spot viewed by the pyrometer and we therefore believe it to be an artifact. The true temperatures calculated for these experiments under the assumption of a grey emissivity model fit well

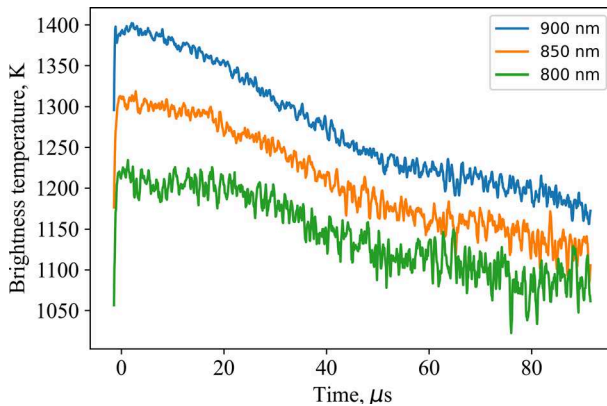


Fig. 5 Brightness temperature curves for copper foil heated by lead ion beam (shot #365°, 90° angle between the pyrometer and the surface)

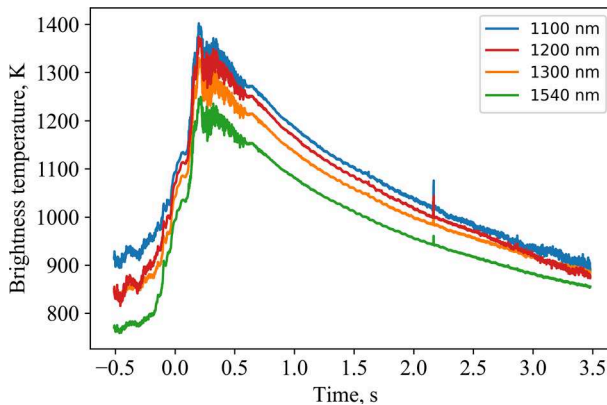


Fig. 6 Brightness temperature curves of a pyrotechnic sparkler

with the expected surface temperature of a sparkler, which is close to 1873 K [9]. This experiment demonstrates that the developed modular pyrometer is also suitable for temperature measurements of exothermic processes where moderately high temperatures are reached within a few seconds.

4 Data Analysis Methods

Theoretical predictions of the spectral emissivity of a sample at high temperatures are extremely challenging and generally not very reliable due to multiple reasons [10]. Therefore, the empirical models for the emissivity introduced above are often used instead.

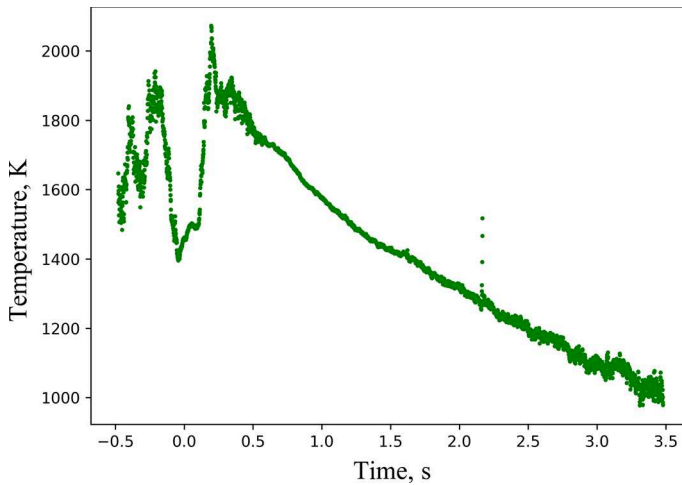


Fig. 7 Typical true temperature curves of a pyrotechnic sparkler

The most widely used model is the grey-body approximation [4, 5], although it provides sufficient accuracy only for certain materials and in a narrow temperature and wavelength range. As the next level, a polynomial (usually linear) dependence of the emissivity on the wavelength is often assumed, or, alternatively, an exponential raised to a polynomial emissivity model [11].

In our experiments, the brightness temperature for each channel has been obtained by calibration. We have used either the grey-body model or the linear wavelength emissivity dependence assumption. More complex emissivity models would not provide a better accuracy due to the limited number of channels and a relatively narrow wavelengths range (800–900 nm) used in our experiments.

The temperature resolution of the pyrometer, defined as the smallest temperature increment that can be resolved, depends mostly on the change of the emitted radiation energy as a function of temperature. The digitization of the analog signals by the oscilloscope also plays a role but can be significantly improved by averaging the signal, at the cost of a limited temporal resolution. The absolute temperature resolution is a function of temperature and the absolute uncertainty increases with increasing temperature.

The absolute temperature accuracy is mainly determined by the calibration, by the quality of the representation of the spectral emissivity of the surface, and also by noise. The temperature of our calibration lamp is accurate within 10 K for temperatures lower than 1873 K and within 8 K for higher temperatures, which is about 0.5 %. The influence of noise is only important for small signal-to-noise ratios, i.e., at low temperatures. For the infrared PIN diodes used in the sparkler experiment the noise voltage equals 2 mV while the typical signal voltage varies from 50 mV to 1 V, so the uncertainty varies from 0.5 % to 4 %. For the fast visible and infrared range PIN diodes output noise equals 20 mV for a 1 V output range, so the uncertainty is always higher than 2 %. The unknown emissivity of the surface can contribute an error of 5 % or higher [12]. In summary, the primary source of the

absolute error for the measured temperature is the unknown surface emissivity at high temperatures and noise at low temperatures.

Figure 7 shows the grey-body temperature of the sparkler (see Sect. 3.3). The true temperature is determined with rather good accuracy during the cooling process, i.e., starting from circa 0.5 s, while before this time the chemical reactions take place at the target surface, and the temperature measurements become problematic. The application of the linear emissivity model gives a very similar result for the true temperature.

However, similar true temperature calculations for the fast heavy-ion experiment using constant and linear emissivity models did not fully agree with each other. The possible reasons for this are the 45° angle of view of the pyrometer due to geometrical constraints inside the target chamber as well as the temperature gradients along the spot size. The emissivity of liquid metals for such light emission direction is unknown and cannot be predicted reliably. Therefore, currently reliable measurements require optical access along the surface normal and the smallest possible observation spot size, i.e., the smallest fiber, which still can provide a reasonably high optical intensity.

5 Conclusion

A fast multichannel pyrometer for high temperature measurements has been designed and successfully tested. Several improvements, including a new calibration lamp and new types of detectors, have substantially enhanced its accuracy up to a few tens of Kelvin, depending on the temperature range and the characteristic time of the experiment.

This final version of the pyrometer uses five wavelength channels in each arm from 500 to 1550 nm, two arms (with different spot positions on the target) simultaneously, and different types of detectors, such as various infrared and visible PIN photodiodes and Multi Pixel Photon Counters (MPPC). This enables temperature measurements in a broad range up to a few thousand Kelvin with a nanosecond temporal resolution.

It was found that modern PIN photodiode detectors such as Femto HCA-S-400 M-IN and Femto HCA-S-400 M-SI are better suited than MPPC for fast multi-wavelength pyrometry measurements on a nanosecond time scale because the measured effective time resolution of MPPC is slightly worse due to their intrinsic noise and relatively low dynamic range.

We have shown that the capabilities of the developed instrument can be used for dynamic ion-heating experiments as well as for any type of “slow” (millisecond) experiments. With only minor modifications, the pyrometer can also be used for other types of experiments, such as temperature determination in laser-heated diamond anvil cell experiments.

The new aspects of the system presented here rest, in part, on the use of MPPCs, which, to the best of our knowledge, have never been used for the pyrometrical applications before. The use of two complementary “arms” and the resultant high degree of flexibility of the system is also novel. Incorporation of state-of-the-art

components, such as detectors (PIN diodes and MPPCs) in conjunction with a high-end oscilloscope provides a unique combination of very high temporal and good temperature resolution.

In comparison to established single- or double-channel pyrometers, our multi-channel pyrometer allows a much more detailed and wavelength- dependent observation of the changes in the emissivity during the experiment. This additional information allows us to explore the use of different kinds of emissivity functions in the data analysis. This is important as it is generally unclear, which emissivity function is best suited for a given experiment, and the multi-channel measurements allow to derive this information with the use of alternative and complementary approaches in the data analysis.

We have very low light intensities in our dynamic experiments in comparison to conventional temperature measurements allowing time averaging, as we need to collect the data on a nanosecond time scale, the signal-to-noise ratio increases with adding more channels. The emissivity can change drastically during the fast experiments in an unpredictable way due to phase transformations (melting, boiling, plasma) and changes of the surface. Here again, three to five channels are found to provide an optimal balance between sensitivity, signal-to-noise ratio, and temporal resolution in the expected temperature range in our experiments.

Acknowledgments This work is supported by the Bundesministerium für Bildung und Forschung der Bundesrepublik Deutschland (BMBF), grant number 05P21RFFA2. The results presented here were partly obtained in the experiment S489 performed at the HHT area of the GSI Helmholtzzentrum für Schwerionenforschung, Darmstadt (Germany) in the frame of FAIR Phase-0 program.

Funding Open Access funding enabled and organized by Projekt DEAL. This work was funded by the Federal Ministry of Education and Research (BMBF), Germany, grant number 05P21RFFA2.

Data Availability The data that support the findings of this study are available from the corresponding author upon reasonable request.

Open Access This article is licensed under a Creative Commons Attribution 4.0 International License, which permits use, sharing, adaptation, distribution and reproduction in any medium or format, as long as you give appropriate credit to the original author(s) and the source, provide a link to the Creative Commons licence, and indicate if changes were made. The images or other third party material in this article are included in the article's Creative Commons licence, unless indicated otherwise in a credit line to the material. If material is not included in the article's Creative Commons licence and your intended use is not permitted by statutory regulation or exceeds the permitted use, you will need to obtain permission directly from the copyright holder. To view a copy of this licence, visit <http://creativecommons.org/licenses/by/4.0/>.

References

1. V. Mintsev, V. Kim, I. Lomonosov, D. Nikolaev, A. Ostrik, N. Shilkin, A. Shutov, V. Ternovoi, D. Yuriev, V. Fortov, A. Golubev, A. Kantsyrev, D. Varentsov, D.H.H. Hoffmann, Non-ideal plasma and early experiments at FAIR: HIHEX—heavy ion heating and expansion. *Contrib. Plasma Phys.* **56**(3–4), 281–285 (2016)
2. A. Araújo, Multi-spectral pyrometry—a review. *Meas. Sci. Technol.* **28**, 082002 (2017)

3. P.A. Ni, M.I. Kulish, V.Y. Mintsev, D.N. Nikolaev, V.Y. Ternovoi, D.H.H. Hoffmann, S. Udrea, A. Hug, N.A. Tahir, D. Varentsov, Temperature measurement of warm-dense-matter generated by intense heavy-ion beams. *Laser Part. Beams* **26**, 583–589 (2008)
4. A. Hug, Thermodynamic properties of heavy ion heated refractory metals. PhD thesis, Darmstadt (2011)
5. P. Ni, Temperature measurement of high-energy-density matter generated by heavy ion beam. PhD thesis, Darmstadt (2006)
6. E.M. Vuelban, F. Girard, M. Battuello, P. Nemecek, M. Maniur, P. Pavlasek, T. Paans, Radiometric techniques for emissivity and temperature measurements for industrial applications. *Int. J. Thermophys.* **36**, 1545–1568 (2015)
7. P.A. Ni, R.M. More, H. Yoneda, F.M. Bieniosek, Polarization pyrometry: an improvement to multi-wavelength optical pyrometry. *Rev. Sci. Instrum.* **83**(123501), 1–6 (2012)
8. L.N. Latyev, V.A. Petrov, V.Ya. Chekhovskoy, E.N. Shestakov, Radiating Properties of Solid Materials: Hand-Book. Energia, Moscow (1974)
9. P.J. Disimile, R. Prasad, N. Toy, Temperature measurements within the luminous region of a burning Ba(NO₃)/Al mixture. *J. Pyrotech.* **23**, 10–20 (2006)
10. C. Rodiet, B. Remy, A. Degiovanni, F. Demeurie, Optimization of the wavelength range and number of bands used for the multi-spectral temperature measurement of surfaces exhibiting nonuniform emissivity, 1978. Paper presented at the 11th International Conference on Quantitative Infrared Thermography, Naples, Italy (2012)
11. M.A. Khan, Ch. Allemand, Th. Eagar, Noncontact temperature measurement. II. Least squares based techniques. *Rev. Sci. Instrum.* **62**, 403–409 (1991)
12. B. Müller, U. Renz, Development of a fast fiber-optic two-color pyrometer for the temperature measurement of surfaces with varying emissivities. *Rev. Sci. Instrum.* **72**(8), 3366–3374 (2001)

Publisher's Note Springer Nature remains neutral with regard to jurisdictional claims in published maps and institutional affiliations.